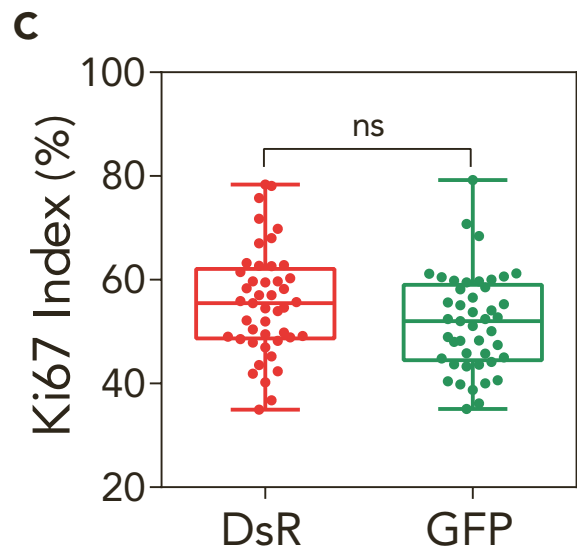
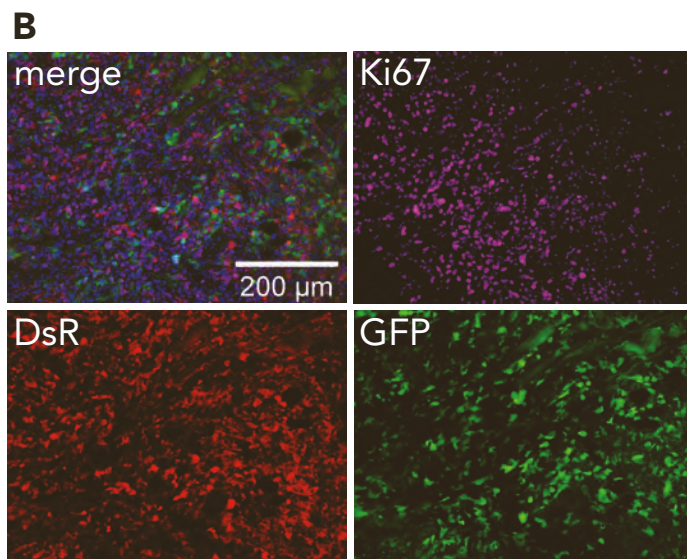
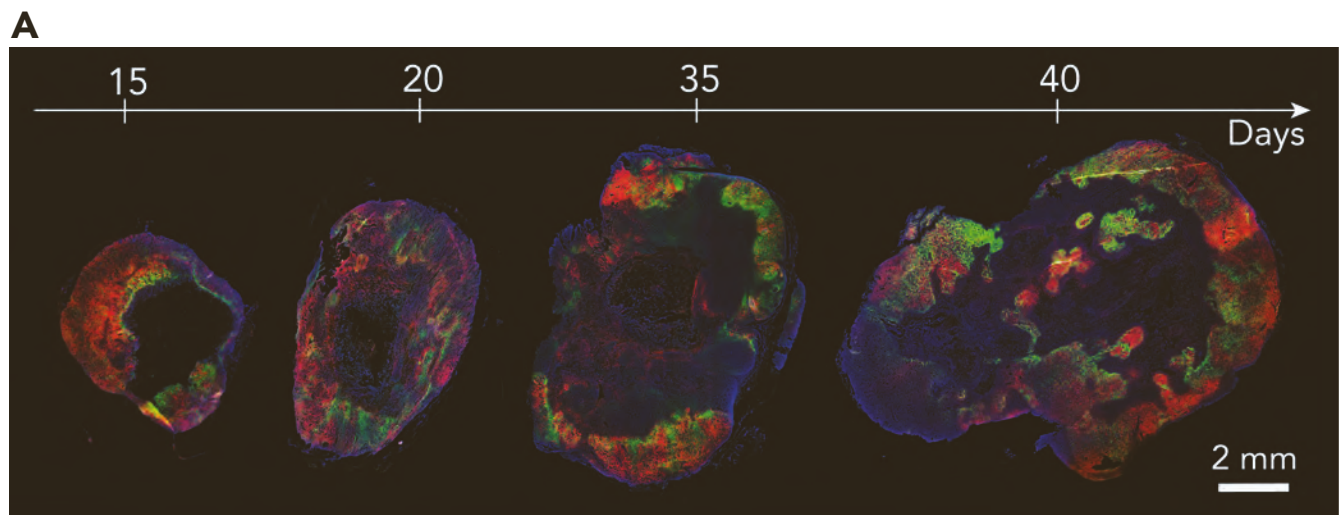


**iScience, Volume 24**

**Supplemental information**

**A persistent invasive phenotype in post-hypoxic  
tumor cells is revealed by fate mapping  
and computational modeling**

**Heber L. Rocha, Inês Godet, Furkan Kurtoglu, John Metzcar, Kali  
Konstantinopoulos, Soumitra Bhoyar, Daniele M. Gilkes, and Paul Macklin**



**Figure S1. Fate-mapping intratumoral hypoxia and proliferation analysis, Related to Figure 2.** (A) Fluorescent images of the full cross-sections of orthotopic tumors derived from MDA-MB-231 hypoxia fate-mapping cells. Tumors were excised at days 15, 20, 35 and 40 of the time course. (B-C) Representative fluorescent image (B) and quantification (C) of Ki67 staining in DsRed+ and GFP+ cells in a tumor section.

Parameter	Meaning	Value	Reference
$U$	oxygen consumption rate by cells	$10 \text{ min}^{-1}$	Ghaffarizadeh <i>et al.</i> 2016
$D$	oxygen diffusion coefficient	$10^5 \mu\text{m}^2/\text{min}$	Ghaffarizadeh <i>et al.</i> 2016
$\lambda$	oxygen natural decay	$0.1 \text{ min}^{-1}$	Ghaffarizadeh <i>et al.</i> 2016
$\sigma_0$	initial oxygen pressure	$45.94 \text{ mmHg}$	Estimated
$\bar{\sigma}$	oxygen pressure at the edges of tumor	$45.94 \text{ mmHg}$	Godet <i>et al.</i> 2019
Initial_radius	radius of the initial tumor	$250 \mu\text{m}$	Estimated
$\bar{r}_{01}$	transition rate from Ki67- to Ki67+	$3.63 \times 10^{-3} \text{ min}^{-1}$	Ghaffarizadeh <i>et al.</i> 2018
$r_{10}$	transition rate from Ki67+ to Ki67-	$1.07 \times 10^{-3} \text{ min}^{-1}$	Ghaffarizadeh <i>et al.</i> 2018
$\sigma_S$	oxygen pressure threshold to signal proliferation saturation	$38 \text{ mmHg}$	Estimated
$\sigma_T$	min oxygen pressure threshold to signal proliferation	$6 \text{ mmHg}$	Estimated
$\sigma_H$	oxygen pressure threshold to signal hypoxia	$10 \text{ mmHg}$	Godet <i>et al.</i> 2019
$\alpha_i$	protein production rate	$4.8 \times 10^{-4} \text{ min}^{-1}$	Estimated
$\beta_i$	protein degradation rate	$6.9 \times 10^{-5} \text{ min}^{-1}$	Estimated

**Table S1. Parameter values utilized in the simulations of the computational model, Related to Figure 4.**

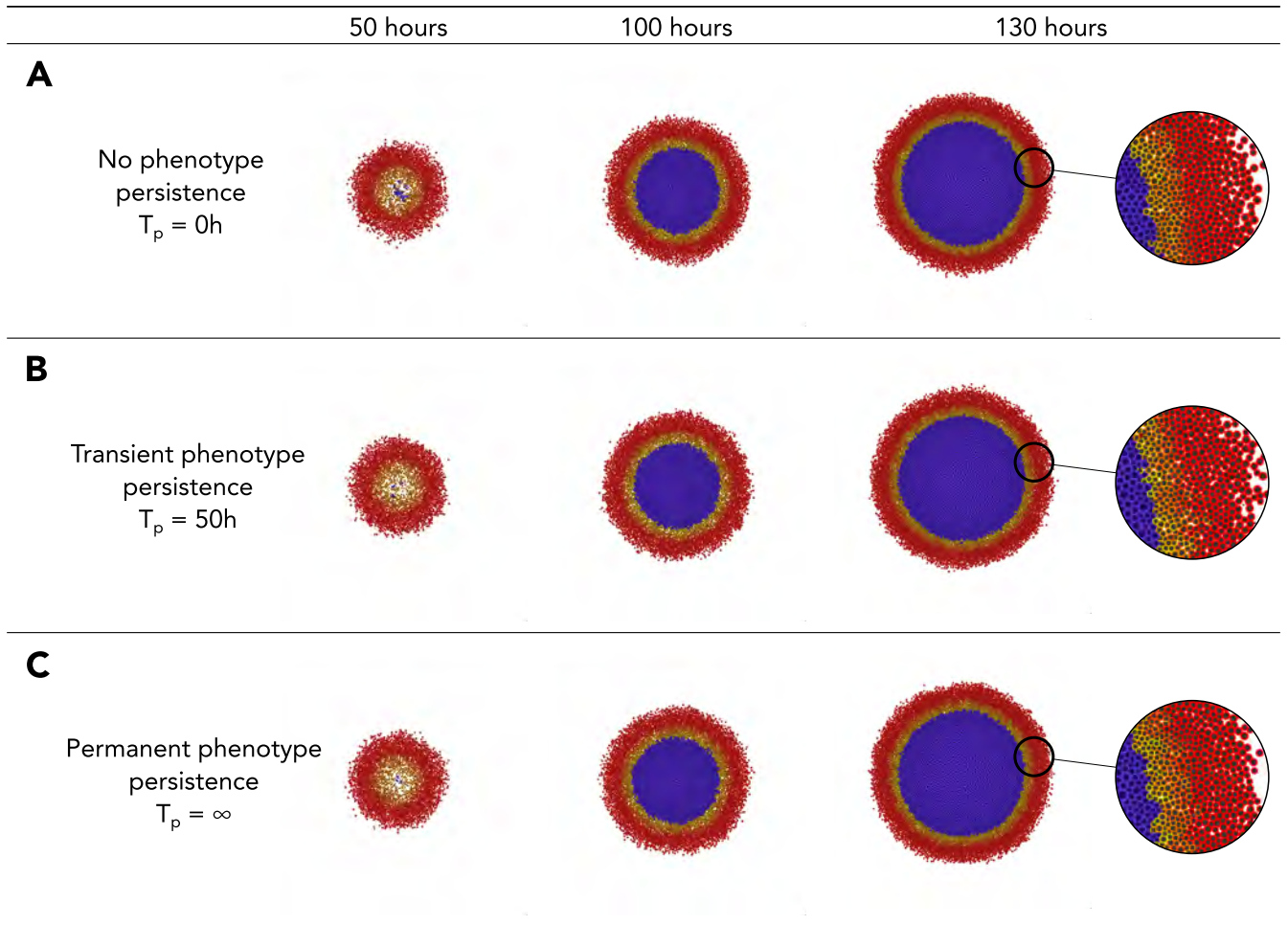


**Figure S2. Impact of phenotypic persistence time with migratory bias fixed ( $b = 0.1791$ ), Related to Figure 4. (A) No phenotypic persistence ( $T_p = 0$ ). (B) Intermediate phenotypic persistence ( $T_p = 50 \text{ h}$ ). (C) Permanent phenotypic persistence ( $T_p = \infty$ ).**

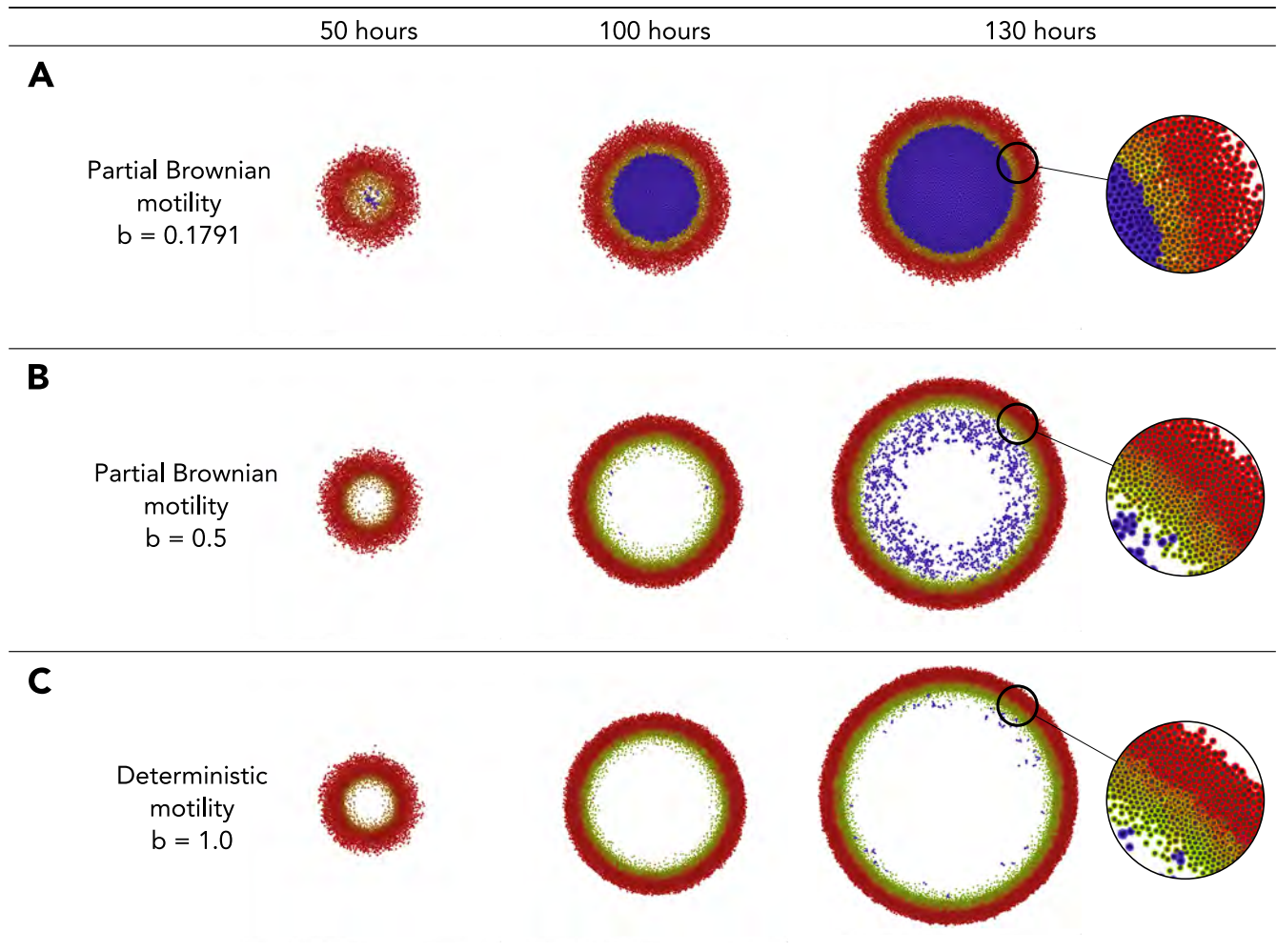


**Figure S3. Impact of migratory bias without phenotypic persistence ( $T_p = 0$ ), Related to Figure 4.** (A) The motility bias generates a partial Brownian motility ( $b = 0.1791$ ). (B) Intermediate motility bias achieves a more directed migration ( $b = 0.5$ ). (C) Completely polarized movement ( $b = 1.0$ ).

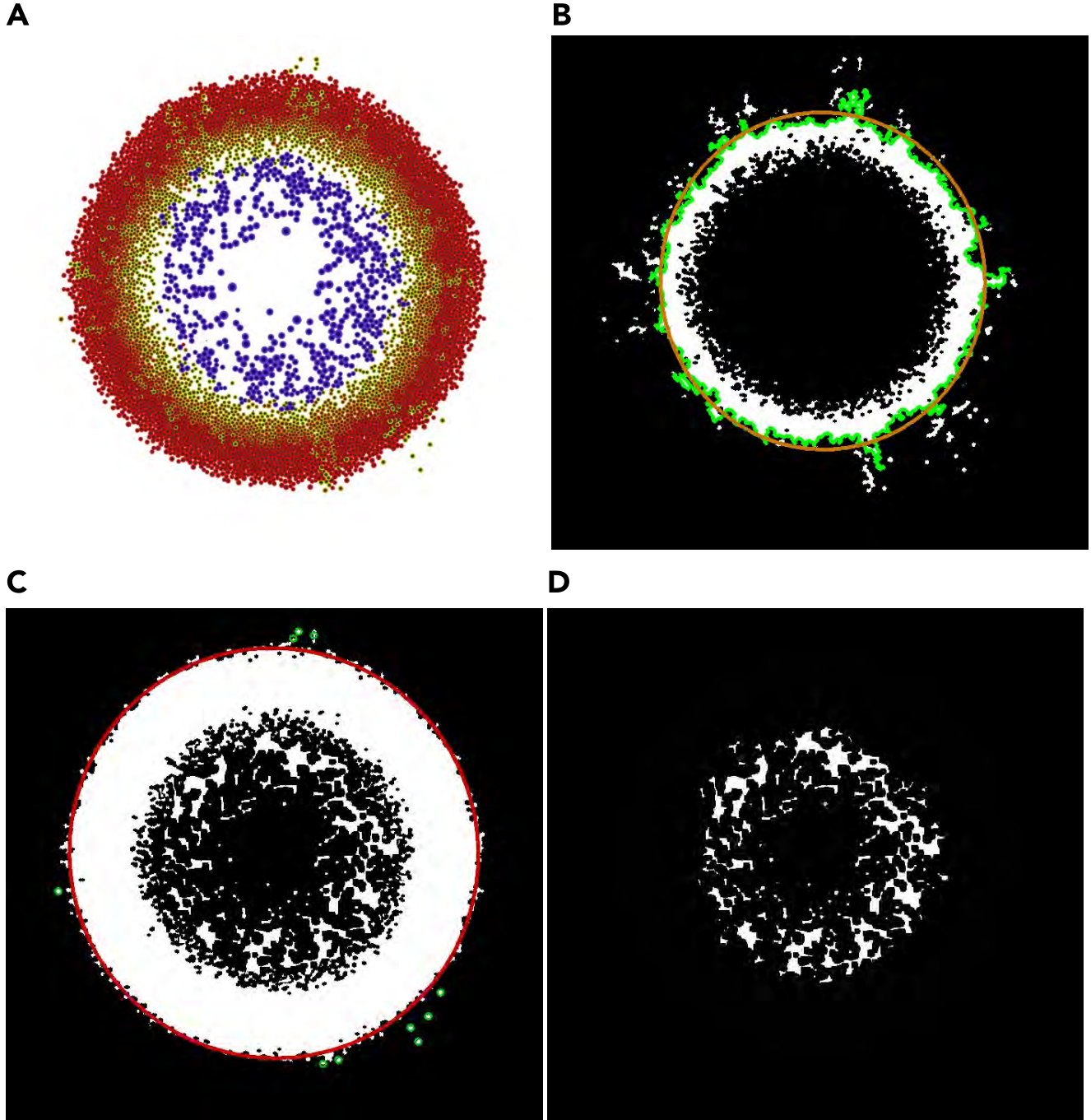


**Figure S4. Image classifier output, Related to STAR Methods.** (A) Output of the model using one simulation of the model at 100 hours with  $F_r = 50\%$ ,  $b^* = 0.5$ , and  $T_p = 50h$ . (B) Image of the Boolean test for plumes. The function  $\mathcal{F}_G$  in green and ellipse  $\mathcal{E}_G$  in orange. (C) Image of the Boolean test for escaping cells. The ellipse  $\mathcal{E}_T$  fitting the tumor in red, and the GFP+ cells escaping the tumor in green. (D) Image of necrotic area.

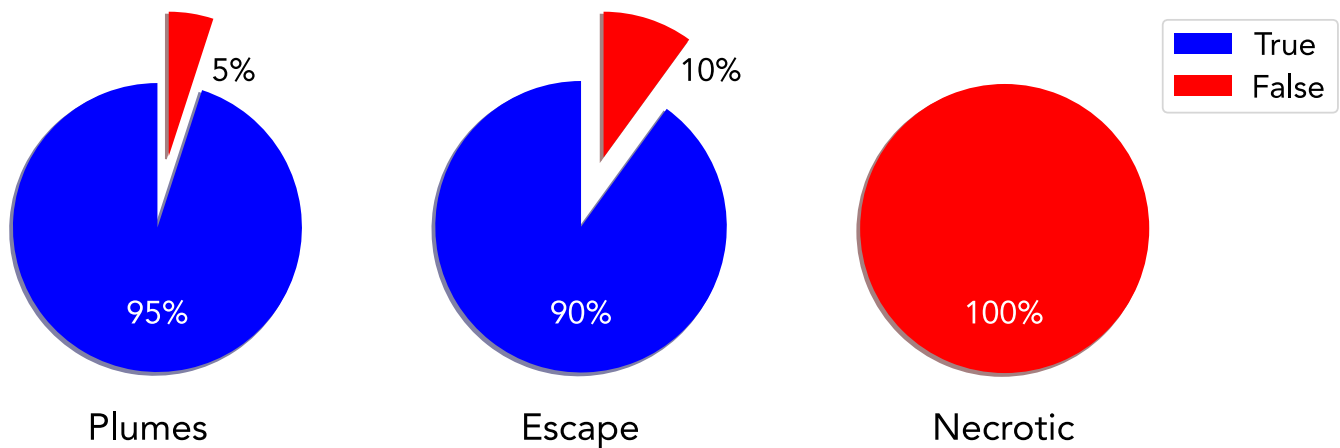


**Figure S5. Boolean image classification, Related to STAR Methods.** Percentage of the Boolean image classification of 20 replicates of the model (associated to 100h of tumor evolution), when  $F_r = 50\%$ ,  $b^* = 0.5$ , and  $T_p = 50h$ .

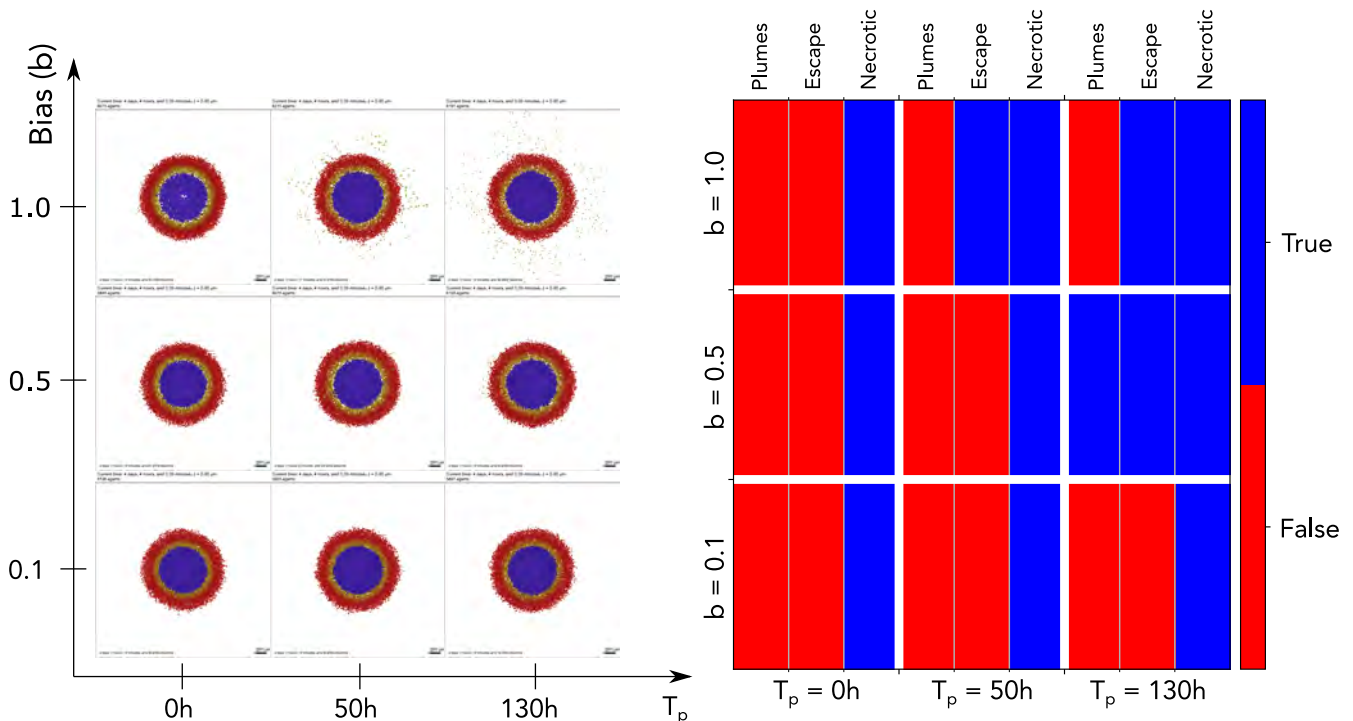


**Figure S6. Study varying  $b$  and  $T_p$  with  $F_r = 10\%$ , Related to STAR Methods.** Images resultant from the proposed model (left) and associated Boolean classification (right). All simulations were evaluated at 100 hours after the initial condition.

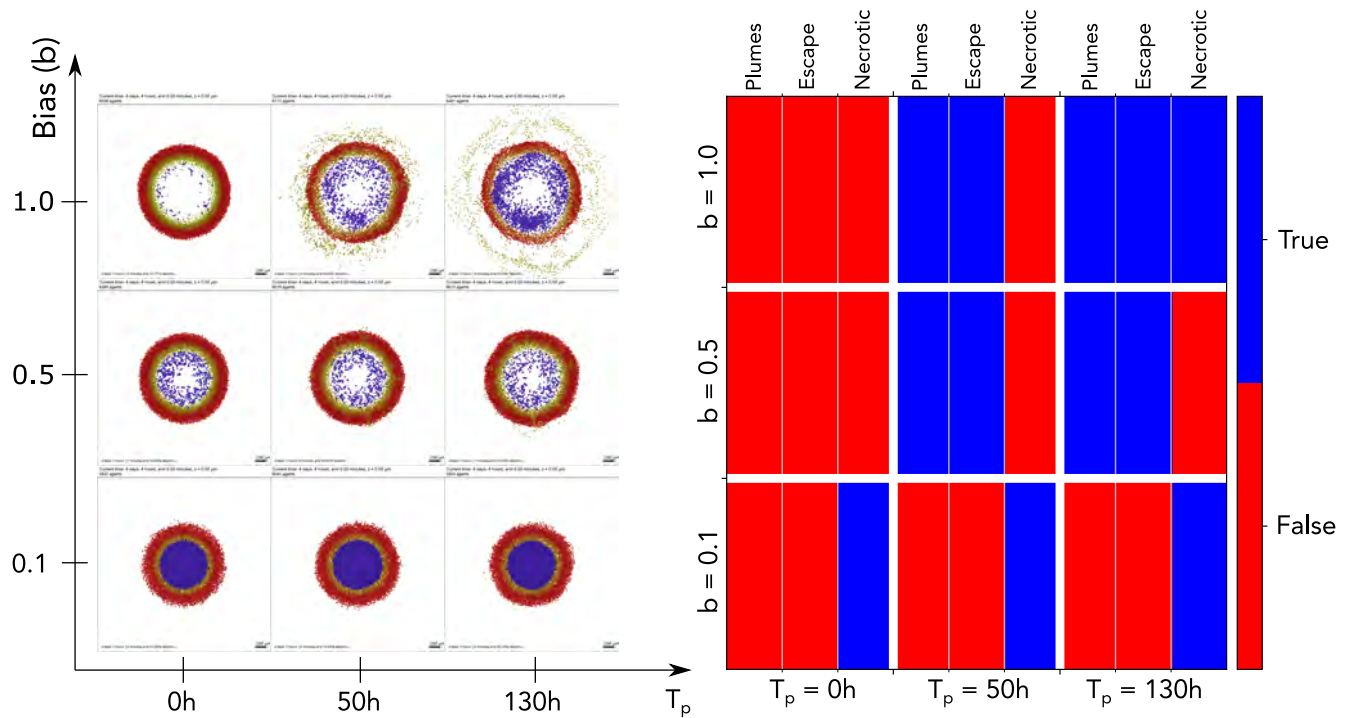


**Figure S7. Study varying  $b$  and  $T_p$  with  $F_r = 50\%$ , Related to STAR Methods.** Images resultant from the proposed model (left) and associated Boolean classification (right). All simulations were evaluated at 100 hours after the initial condition.

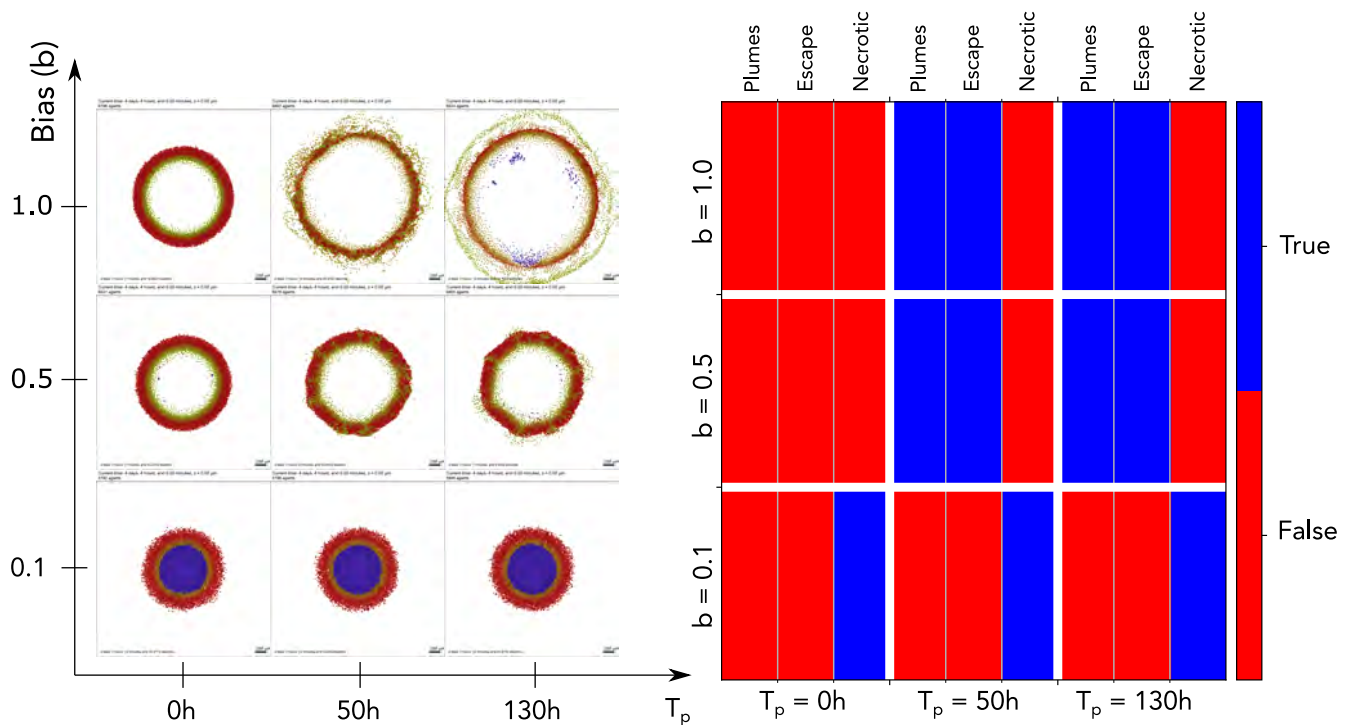


**Figure S8. Study varying  $b$  and  $T_p$  with  $F_r = 100\%$ , Related to STAR Methods.** Images resultant from the proposed model (left) and associated Boolean classification (right). All simulations were evaluated at 100 hours after the initial condition.

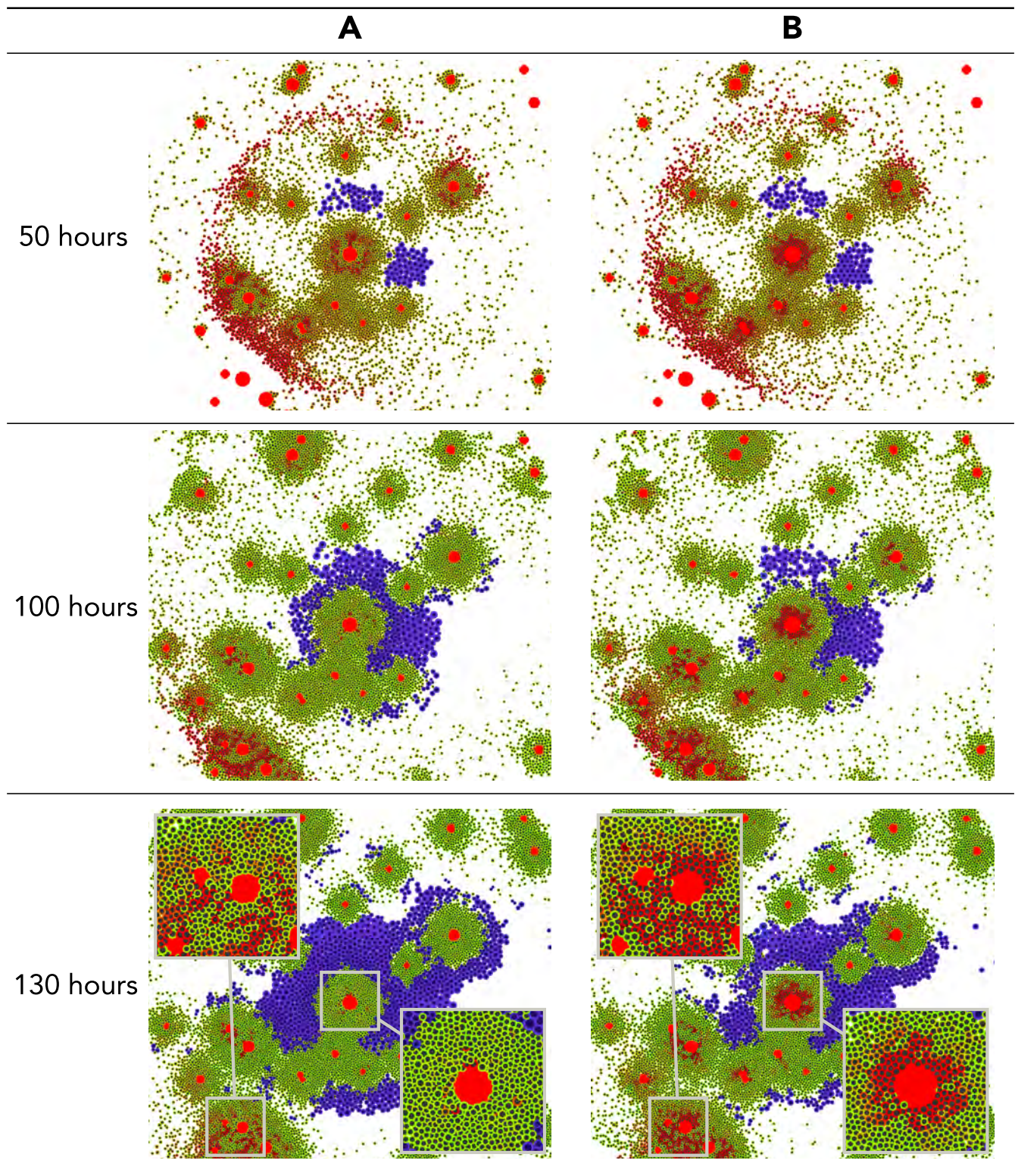


**Figure S9. Impact of heterogeneous and multiple oxygen sources, Related to STAR Methods.** (A-B) The simulation of the model for the case in which we arranged oxygen sources randomly in the computational domain, (A) adopting  $F = 50$ ,  $b = 0.5$ , and  $T_p = 50 h$ ; and (B) adding mechanical feedback on proliferation and migration.